Journal of
NANOSTRUCTURES
JNS
NANOSTRUCTURES
JNS.kashanu.ac.ir

Synthesis Magnesium Hydroxide Nanoparticles and Cellulose Acetate-$Mg(OH)_2$-MWCNT Nanocomposite

M. Ghorbanali [a], A. Mohammadi [b], R. Jalajerdi [c]*

[a] *Faculty of Graphic, Higher Education Institute of Art Allameh Bahrololoom, Boroujerd, Iran*

[b] *Advertising Engineering BRS Academy, New York, USA*

[c] *Young Researchers and Elite Club, Arak Branch, Islamic Azad University, Arak, Iran*

Article history:
Received 11/04/2015
Accepted 19/05/2015
Published online 01/06/2015

Keywords:
Nanoparticles
Nanocomposite
Thermal Stability
Cellulose Acetate

**Corresponding author:*
E-mail address:.
Jalajerdi@gmail.com
Phone: +98 863256414
Fax: +98 863256414

Abstract

$Mg(OH)_2$ nanoparticles were synthesized by a rapid microwave reaction. The effect of sodium dodecyl sulfonate (SDS as anionic surfactant) and cetyl tri-methyl ammonium bromide (CTAB as cationic surfactant) on the morphology of magnesium hydroxide nanostructures was investigated. Multi wall carbon nano tubes was organo-modified for better dispersion in cellulose acetate matrix. The influence of $Mg(OH)_2$ nanoparticles and modified multi wall carbon nano tubes (MWCNT) on the thermal stability of the cellulose acetate (CA) matrix was studied using thermo-gravimetric analysis (TGA). Nanostructures were characterized by X-ray diffraction (XRD), scanning electron microscopy (SEM) and Fourier transform infrared (FT-IR) spectroscopy. Thermal decomposition of the nanocomposites shift towards higher temperature in the presence of $Mg(OH)_2$ nanostructures. The enhancement of thermal stability of nanocomposites is due to the endothermic decomposition of $Mg(OH)_2$ and release of water which dilutes combustible gases.

1. Introduction

Applying of halogen-free flame retardants is widespread due to the increasing concern about the health and environmental risks [1-3]. One of the most commonly used mineral flame retardants is magnesium hydroxide. As the temperature rises magnesium hydroxide shows an endothermic decomposes (1.356 kJ/g) around 330°C and absorbs energy. Moreover, it releases non-flammable water which dilutes highly flammable gases. Magnesium hydroxide is used as halogen-free flame-retardant for polymers. $Mg(OH)_2$ can act also as a reinforcing agent, flame retardant and smoke suppressant additive with low or zero emissions of toxic or hazardous substances [1–5]. The main advantages of polymeric materials over many metal compounds

are high toughness, corrosion resistance, low density and thermal insulation. Improvement of the flame retardancy and thermal stability of polymers is a major challenge for extending their use for most applications. One of the main drawback of magnesium hydroxide is that for effective flame retardancy tests high loading levels are required to achieve the appropriate fire retardancy. Increasing the loading of inorganic metal hydroxides will result in a significant decrease in physical properties. The higher level of flame retardancy of nanoparticles is due to their bigger surface to volume fractions which let them disperse into the polymeric matrix homogeneously, and hence leads to formation of a compact char during the combustion [6-11]. Cellulose acetate has been used in a wide range of applications due to its particular advantages. It is a biodegradable polymer with applications in photographic, paper coating, packaging films and adhesives. The physical and chemical properties of nanoparticles are greatly influenced by their shape and size distribution as well as their agglomerated state and dispersion property, which are strongly related to the preparation process [12-17].. In this work a facile and rapid method for preparation of magnesium hydroxide was used. Magnesium hydroxide and modified carbon nano tubes were then added to the cellulose acetate in order to increase the thermal stability and flame retardancy.

2 Experimental

2.1 Materials and characterization

$Mg(NO_3)_2$ $6H_2O$, ammonia, ethylene glycol, sodium dodecyl sulfonate (SDS), cetyl tri-methyl ammonium bromide (CTAB) were purchased from Merck and cellulose acetate (CA) from Sigma-Aldrich. All the chemicals were used as received without further purifications. Nanocyl™ NC 7000 is the name of Nanocyl's innovative Multiwall Carbon Nanotubes.

Scanning electron microscopy (SEM) images were obtained using a LEO instrument (Model 1455VP). Prior to taking images, the samples were coated by a very thin layer of Au (BAL-TEC SCD 005 sputter coater) to make the sample surface conducting obtain better contrast and prevent charge accumulation. In UL-94 a bar shape specimen of plastic 127 × 12.7 × 1.6 mm is positioned vertically and held from the top. A Bunsen burner flame is applied to the specimen twice (10 s each). X-ray diffraction (XRD) patterns were recorded by a Philips X-ray diffractometer using Ni-filtered CuK_α radiation. For preparation of nanocomposite, a multi-wave ultrasonic generator (Bandeline MS 73) equipped with a converter/transducer and titanium oscillator operating at 20 kHz with a maximum power output of 100 W was used for the ultrasonic irradiation. The effect of nanostructure on flame retardant properties has been considered using UL-94 test. In UL-94 a bar shape specimen of plastic 127 × 12.7 × 1.6 mm is positioned vertically and held from the top. A Bunsen burner flame is applied to the specimen twice (10 s each). A V-0 classification is given to material that is extinguished in less than 10 s after any flame application, drips of particles allowed as long as they are not inflamed. A V-1 classification is received by a sample with maximum combustion time < 30 s, drips of particles allowed as long as they are not inflamed. The sample is classified V-2 if it satisfies the combustion time criteria of V-1, but flaming drips are allowed. Materials are ranked as N.C. in UL-94 tests when the maximum total flaming time is above 50 s. The sample is classified HB when slow burning on a horizontal specimen; burning rate < 76 mm/min [14-17].

2.2. Synthesis of $Mg(OH)_2$ nanoparticles

1g $Mg(NO_3)_2$ $6H_2O$ and 0.2 g of surfactant were dissolved in ethylene glycol. 20 mL of ammonia (12 M), was slowly added into the solution under microwave irradiation at 750 W (5 minutes, 40s on : 60s off). The white precipitate was centrifuged and washed with distilled water to removing the surfactant, and later dried at 70°C for 24h in a vacuum dryer. These stages carried out for four surfactant materials as synergetic additives including CTAB and SDS.

2.3. Synthesis of CA-$Mg(OH)_2$ nanocomposite

4 g of CA was dissolved in 15 mL of acetone and then $Mg(OH)_2$ (0.8 g) and MWCNT (0.2) were dispersed in 5 mL of acetone with ultrasonic waves (60W, 30 min). The dispersion of $Mg(OH)_2$ was then added slowly to the polymer solution. The solution was mixed under stirring for 6 h.

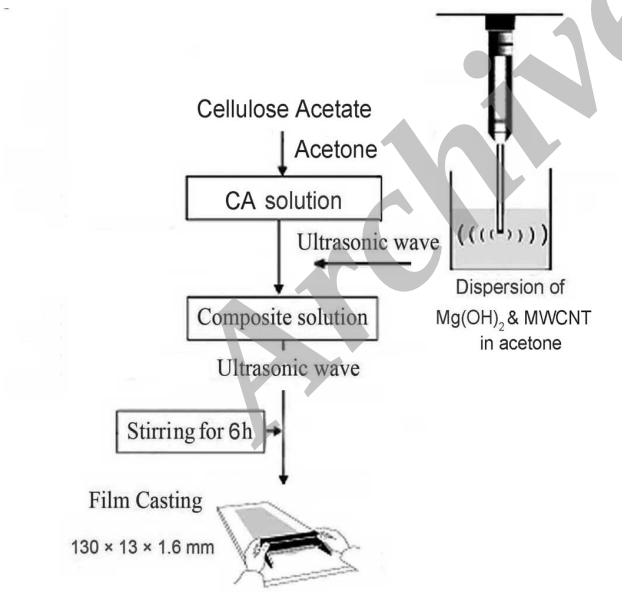

Fig. 1. Preparation of CA-$Mg(OH)_2$ nanocomposite

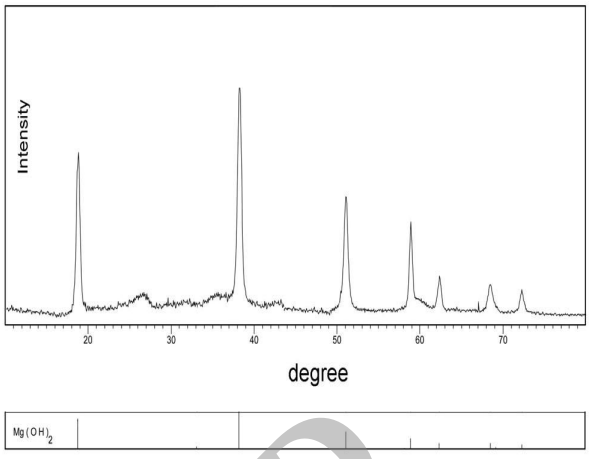

Fig. 2. XRD pattern of $Mg(OH)_2$ nanoparticles

For preparation of samples for UL-94 test after stirring, the product was casted on a template with dimension 127 × 12.7 mm and after about 48 h of solvent evaporation; the nanocomposite was placed in the vacuum oven for another 6 h for removal of residual traces of water. The final sheets for the test are 127 × 12.7 × 1.6 mm in dimension (stay at oven 90 °C for 48 h) (Fig. 1).

3. Results and discussion

XRD pattern of $Mg(OH)_2$ nanoparticles is shown in Fig. 2. It is indexed as a pure hexagonal structure with suitable agreement to literature value (reference peaks are also depicted in the XRD pattern, JCPDS card no. 78-0316, Space group: P-3m1).

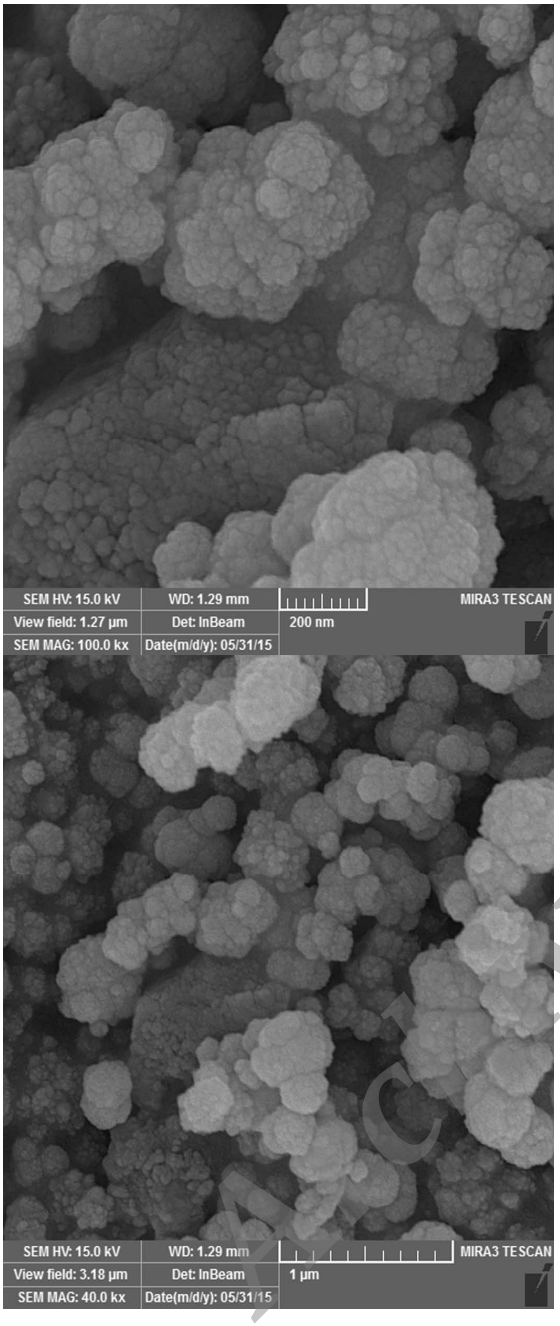

Fig. 3. SEM images of nanoparticles synthesized by SDS

By applying sodium dodecyl sulfonate (SDS as an anionic surfactant, Fig. 3) nanoparticles with mediocre size of 30 nm were synthesized.

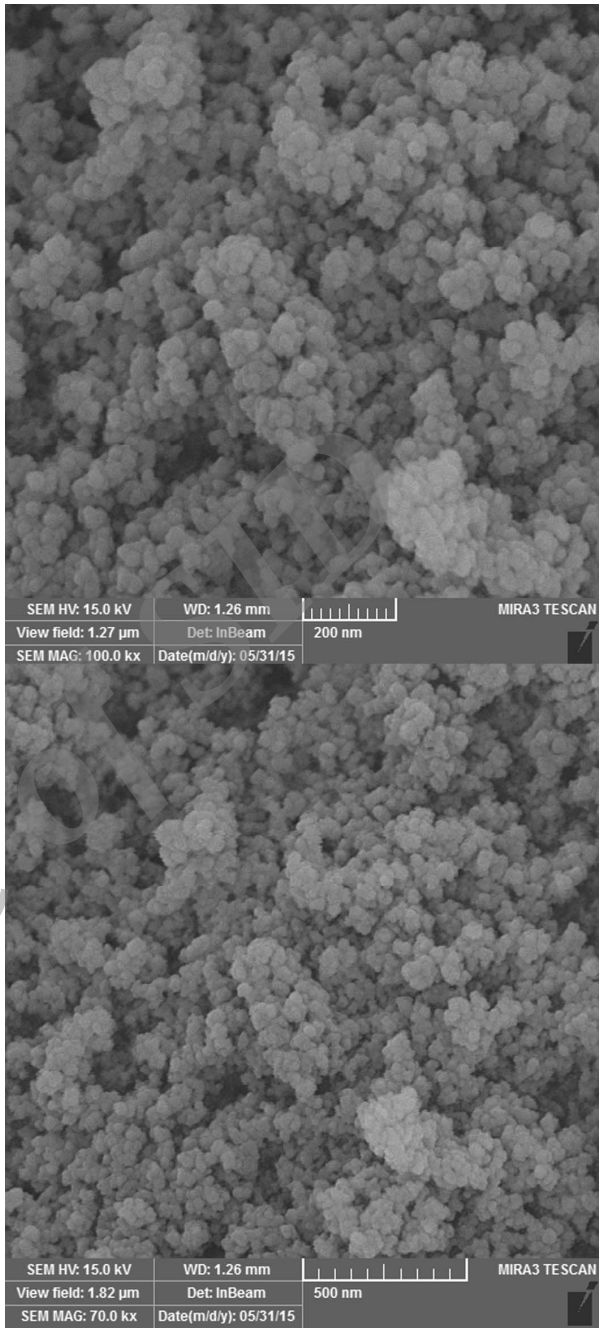

Fig. 4. SEM images of $Mg(OH)_2$ nanoparticles obtained by CTAB

SEM images of $Mg(OH)_2$ synthesized by different surfactants cationic and anionic are shown in Fig. 3-4 respectively. By using cetyl tri-methyl ammonium bromide (CTAB: as a cationic surfactant) nanoparticles with average diameter of 15 nm were obtained (Fig. 4). Surfactant as a capping agent lead

to nucleation step becomes predominant compare to growth stage.

SEM images of modified MWCNTs are shown in Fig 5 that confirm diameter of carbon nanotubes are less than 100 nm. Modified CNT were prepared by carboxylation of nanotubes by applying sulfuric acid and nitric acid simultaneously.

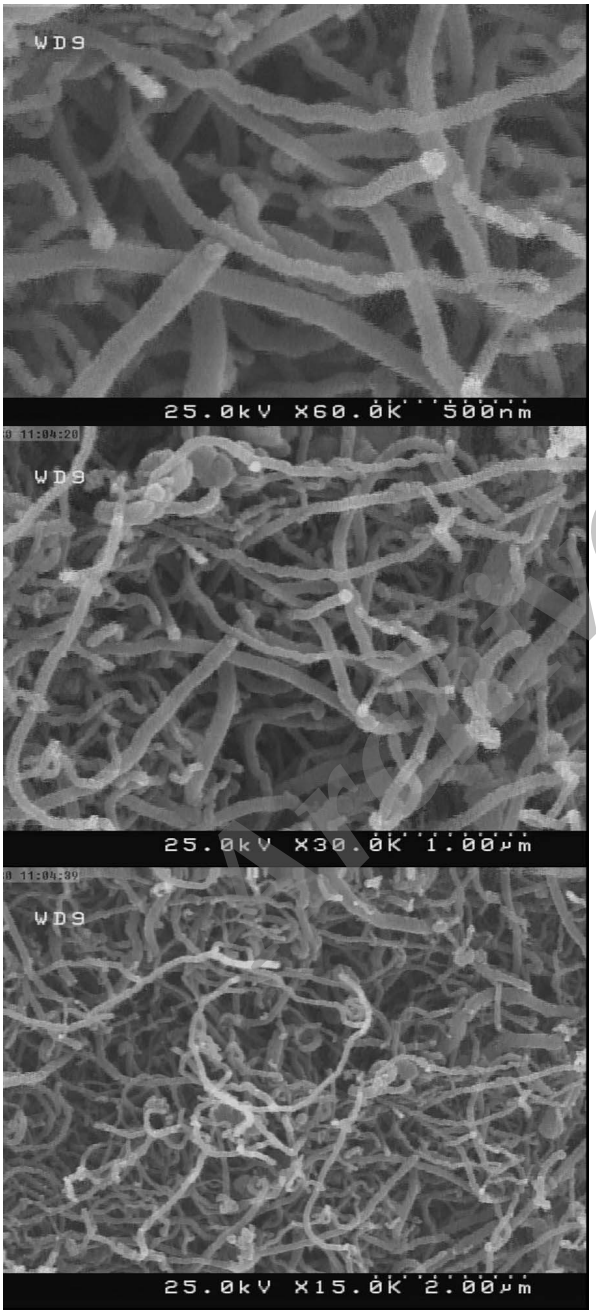

Fig. 5. SEM images of MWCNT

TGA graphs of pure CA and CA-MWCNT-$Mg(OH)_2$ nanocomposite are illustrated in Fig. 6a and 6b respectively. Regarding to curves thermal decomposition of CA-MWCNT-$Mg(OH)_2$ shifts towards higher temperature in presence of metal hydroxide and onset degradation temperature was increased in compare with pure polymer.

The enhancement of thermal stability of nanocomposites is because of endothermic decomposition of $Mg(OH)_2$ that absorbs energy. It simultaneously releases water which dilutes combustible gases. Dispersed nano-tubes and $Mg(OH)_2$ have also a obstruction effect to decrease product volatilization and thermal transport among decomposition of the polymer. Adsorption of polymer chains onto the surface of $Mg(OH)_2$ nanoparticles and nano tubes results in a confinement of the segmental motions and suppress chain-transfer reactions [1-3]. Because of the presence of magnesium hydroxide (endothermic decomposition and absorbs energy) differential thermal analysis of the nanocomposite shows endothermic peaks [1].

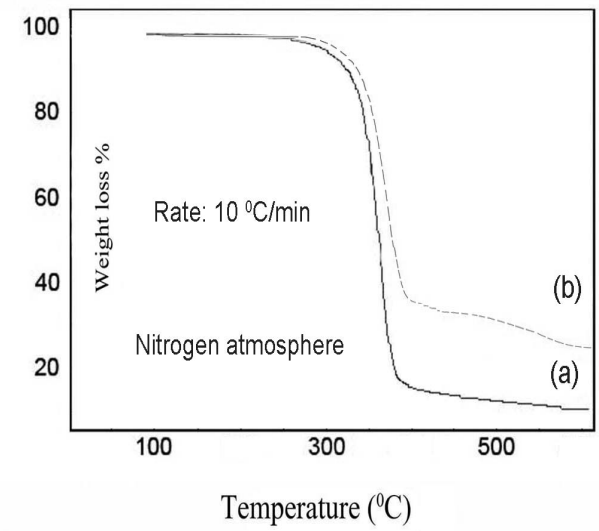

Fig. 6. TGA graphs of (a) pure CA (b) CA-MWCNT-$Mg(OH)_2$ nanocomposite

In CA-MWCNT-$Mg(OH)_2$, nanoparticles and nanotubes have been appropriately distributed in CA matrix and because of hydrogen bonds between them a suitable barrier layer of nanoparticles is formed.

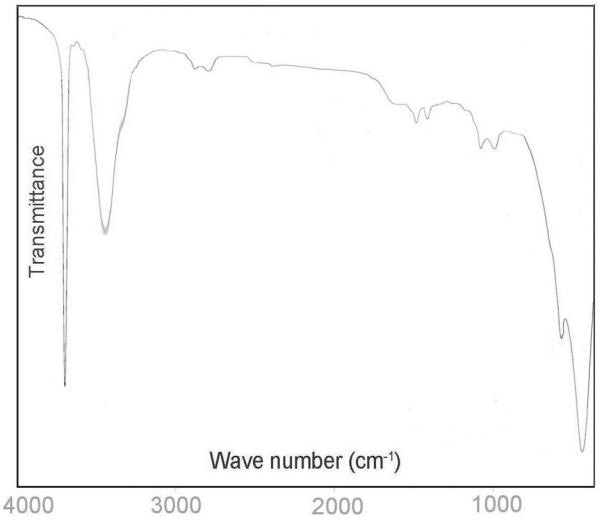

Fig. 7. FT-IR of $Mg(OH)_2$ nanoparticles

UL-94 analysis for CA and CA-$Mg(OH)_2$ nanocomposites are HB and V-0 respectively. The outcomes show that the $Mg(OH)_2$ nanostructure can enhance the flame retardant property of the CA matrix. In the presence of flame nanoparticles make a barrier, this obstacle slows evaporation of polymeric segments and prevents oxygen and flame reaching to the protected sample.

FT-IR spectrum of the $Mg(OH)_2$ is depicted in Fig. 7; absorption at 3410 cm^{-1} is related to O-H bond of adsorbed water. Peak at 3668 cm^{-1} is attributed to the O–H bond stretching vibration in the crystal structure. Absorption at around 419 cm^{-1} is assigned to the Mg–O stretching vibration in $Mg(OH)_2$ [1].

4. Conclusion

$Mg(OH)_2$ nanostructures were prepared by a rapid microwave method. The effect of various surfactants such as SDS and CTAB on the morphology of magnesium hydroxide nanostructures was investigated. $Mg(OH)_2$ nanoparticles and modified MWCNT were then added to cellulose acetate matrix. The influence of the metal hydroxide on the thermal properties of CA was studied using thermo-gravimetric analysis. Thermal decomposition of the CA nanocomposite shift towards higher temperature in the presence of $Mg(OH)_2$ nanoparticles. The increase in flame retardancy of the nanocomposites is due to endothermic decomposition of $Mg(OH)_2$ and release of water which dilutes combustible gases. $Mg(OH)_2$ and MWCNT have also obstruction effect to decrease the polymer volatilization and heat transport during decomposition of the polymer.

References

[1] M. Yousefi, J Nano Struc. 4, (2014) 383-388
[2] D. Ghanbari, M. Salavati-Niasari M. Sabet. Composites: Part B 45 (2013) 550–555.
[3] AB. Morgan, CA. Wilkie, Flame retardant polymer nanocomposite. John Wiley & Sons; New Jersey 2007.
[4] D. Ghanbari, M. Salavati-Niasari, M. Sabet, J Clust Sci. 23 (2012) 1081-1095.
[5] H.R. Momenian, M. Salavati-Niasari, D. Ghanbari, B. Pedram, F. Mozaffar, S. Gholamrezaei, J Nano Struc. 4 (2014) 99-104
[6] H.R. Momenian, S. Gholamrezaei, M. Salavati-Niasari, B. Pedram , F. Mozaffar , D. Ghanbari, J Clust Sci 24 (2013) 1031-1042
[7] D. Ghanbari, M. Salavati-Niasari J Indus Eng Chem. 24 (2015) 284-292.
[8]. C. Henrist, J. P. Mathieu, C. Vogels, A. Rulmont, R. Cloots, J. Cryst. Growth 249 (2003) 321–330.

[9]. F. Laoutid, L. Bonnaud, M. Alexandre, J. Lopez-Cuesta, Ph Dubois, Mater. Sci. Eng. R 63 (2009) 100–125.
[10]. C. S. Choi, B. J. Park, and H. J. Choi, Diam. Relat. Mater. 16 (2007) 1170–1173.
[11]. W. J. Grigsby, C. J. Ferguson, R. A. Franich, G. T. Russell, Int. J. Adhes. Adhes. 25 (2005) 127–137.
[12]. H. Wang, P. Fang, Z. Chen, S. Wang, Appl. Surf. Sci. 253 (2007) 8495–8499.
[13]. J. Kuljanin, M. I. Comor, V. Djokovic, and J. M. Nedeljkovic, Mater. Chem. Phys. 95 (2006) 67–71.
[14] D. Ghanbari, M. Salavati-Niasari, S. Karimzadeh, S. Gholamrezaei, J Nano Struc. 4, (2014) 227-232
[15] P. Jamshidi, D. Ghanbari, M. Salavati-Niasari, J Indus Eng Chem, 20 (2014) 3507-3512.
[16] F. Gholamian, M. Salavati-Niasari, D. Ghanbari, M. Sabet, J Clust Sci 24 (2013) 73–84.
[17] L. Nejati-Moghadam, D. Ghanbari, M. Salavati-Niasari, A. Esmaeili-Bafghi-Karimabad, S. Gholamrezaei, J. Mater. Sci. Mater. Electron. (2015, in press). doi:10.1007/s10854-015-3185-y